INFECTION AND IMMUNITY, June 2004, p. 3204–3217 Vol. 72, No. 6
0019-9567/04/$08.00+0 DOI: 10.1128/IAI.72.6.3204–3217.2004

Virulent and Avirulent Strains of *Francisella tularensis* Prevent Acidification and Maturation of Their Phagosomes and Escape into the Cytoplasm in Human Macrophages

Daniel L. Clemens,* Bai-Yu Lee, and Marcus A. Horwitz

Division of Infectious Diseases, Department of Medicine, School of Medicine, University of California—Los Angeles, Los Angeles, California 90095-1688

Received 25 November 2003/Returned for modification 30 December 2003/Accepted 13 February 2004

***Francisella tularensis*, the agent of tularemia, is an intracellular pathogen, but little is known about the compartment in which it resides in human macrophages. We have examined the interaction of a recent virulent clinical isolate of *F. tularensis* subsp. *tularensis* and the live vaccine strain with human macrophages by immunoelectron and confocal immunofluorescence microscopy. We assessed the maturation of the *F. tularensis* phagosome by examining its acquisition of the lysosome-associated membrane glycoproteins (LAMPs) CD63 and LAMP1 and the acid hydrolase cathepsin D. Two to four hours after infection, vacuoles containing live *F. tularensis* cells acquired abundant staining for LAMPs but little or no staining for cathepsin D. However, after 4 h, the colocalization of LAMPs with live *F. tularensis* organisms declined dramatically. In contrast, vacuoles containing formalin-killed bacteria exhibited intense staining for all of these late endosomal/lysosomal markers at all time points examined (1 to 16 h). We examined the pH of the vacuoles 3 to 4 h after infection by quantitative immunogold staining and by fluorescence staining for lysosomotropic agents. Whereas phagosomes containing killed bacteria stained intensely for these agents, indicating a marked acidification of the phagosomes (pH 5.5), phagosomes containing live *F. tularensis* did not concentrate these markers and thus were not appreciably acidified (pH 6.7). An ultrastructural analysis of the *F. tularensis* compartment revealed that during the first 4 h after uptake, the majority of *F. tularensis* bacteria reside within phagosomes with identifiable membranes. The cytoplasmic side of the membranes of ~50% of these phagosomes was coated with densely staining fibrils of ~30 nm in length. In many cases, these coated phagosomal membranes appeared to bud, vesiculate, and fragment. By 8 h after infection, the majority of live *F. tularensis* bacteria lacked any ultrastructurally discernible membrane separating them from the host cell cytoplasm. These results indicate that *F. tularensis* initially enters a nonacidified phagosome with LAMPs but without cathepsin D and that the phagosomal membrane subsequently becomes morphologically disrupted, allowing the bacteria to gain direct access to the macrophagic cytoplasm. The capacity of *F. tularensis* to alter the maturation of its phagosome and to enter the cytoplasm is likely an important element of its capacity to parasitize macrophages and has major implications for vaccine development.**

Francisella tularensis is a nonmotile, nonsporulating, gram-negative coccobacillus that causes a zoonotic disease in small animals such as rodents, rabbits, and beavers. Humans acquire tularemia by handling infected animals or by the bite of a blood-sucking insect. The infectivity of *F. tularensis* is remarkable: a subcutaneous inoculation of mice with as few as 0.5 to 4 organisms of the virulent Schu strain leads to a fatal infection in 50% of the animals (5). In addition to causing serious and potentially life-threatening natural infections in humans and animals, *F. tularensis* is also considered a potential agent of bioterrorism (19). There are two main biogroups of *F. tularensis*, namely *F. tularensis* subsp. *tularensis* (type A) and *F. tularensis* subsp. *holarctica* (type B). Type A is found only in North America and is highly virulent. Type B is found both in North America and in Europe and has a lower level of virulence. A partially attenuated live vaccine strain (LVS) was developed from type B and has been used as a vaccine with some success (10). However, the safety of this vaccine for immunocompromised individuals and children is unknown, and it is not currently approved for use in humans in the United States. The development of new strategies for treating or preventing tularemia is hindered by the limited knowledge of the pathogenic mechanisms of *F. tularensis*.

Although *F. tularensis* can be grown in the laboratory on enriched culture media, it is thought that, in natural infections, the bacterium replicates exclusively intracellularly within host cells (35). It is clear that *F. tularensis* grows within host mononuclear phagocytes during natural infections. Early studies using infected guinea pigs (17) and chick embryos (8) documented extensive infections of mononuclear phagocytes as well as other cell types. An immunofluorescence histopathologic study of monkeys infected with the fully virulent Schu strain demonstrated that the bacterium was present within macrophages of respiratory bronchioles (49). A study with the attenuated LVS of *F. tularensis* found the bacterium only within mononuclear phagocytes (35). Mononuclear phagocytes are important both as a site of bacterial replication and as a site of host defense against tularemia. Because macrophages are clearly relevant to human disease, we have studied the interaction of *F. tularensis* with human macrophages, using periph-

* Corresponding author. Mailing address: Division of Infectious Diseases, Department of Medicine, UCLA School of Medicine, CHS 37-121, 10833 LeConte Ave., Los Angeles, CA 90095-1688. Phone: (310) 825-9324. Fax: (310) 794-7156. E-mail: dclemens@mednet.ucla.edu.

eral blood monocyte-derived macrophages (MDM) and a human monocyte-like cell line, THP-1, as our model cells.

Intracellular pathogens follow one of three general pathways within a host cell: (i) the extraphagosomal pathway, in which the pathogen lyses the phagosomal membrane and resides freely in the host cell cytoplasm; (ii) the phagolysosomal pathway, in which the pathogen resides and multiplies in an acidified phagosome that fuses with lysosomes; and (iii) the phagosomal pathway, in which the pathogen resides in a phagosome that does not fuse with lysosomes (30). Examples of intracellular pathogens that have been reported to follow the extraphagosomal pathway by lysing their phagosome include *Trypanosoma cruzi* (37, 48), *Listeria monocytogenes* (24), *Shigella* spp. (16, 42), and some species of *Rickettsia* (50). Examples of pathogens that reside in acidified phagolysosomes include *Coxiella burnetii* (11) and *Leishmania amazonensis*. Pathogens that have been shown to reside in phagosomes that do not fuse with lysosomes at various points in their life cycle in macrophages include *Legionella pneumophila* (29), *Chlamydia psittaci* (52), and *Mycobacterium tuberculosis* (4, 12). Within these three general pathways, individual parasites exhibit additional unique variations that can be distinguished ultrastructurally and in terms of the interactions of the parasite or its vacuole with other host cell organelles and of the membrane trafficking within the host cell. These unique variations that characterize the intracellular compartment and its host cell interactions provide the fundamental basis for understanding the cell biology and pathogenetic mechanisms of intracellular parasites. In the case of *F. tularensis*, very little is known about its intracellular compartment, the pH of the compartment, or the interactions between the compartment and the host cell, and most studies have examined the attenuated *F. tularensis* LVS. No studies of the membrane trafficking interactions of virulent *F. tularensis* subsp. *tularensis* in human macrophages have been reported. We show here that both the attenuated LVS and a virulent recent clinical isolate (RCI) of *F. tularensis* subsp. *tularensis* transiently reside in a nonacidified phagosome with abundant staining for lysosome-associated membrane glycoproteins (LAMPs) but with little or no staining for cathepsin D. The phagosomal membranes acquire a densely staining fibrillar coating on their cytoplasmic aspect and subsequently undergo budding, vesiculation, and morphological disruption, giving the bacteria free access to the cytoplasm.

MATERIALS AND METHODS

Reagents and antibodies. Epon and LR White embedding resins, paraformaldehyde, glutaraldehyde, osmium tetroxide, and propylene oxide were purchased from Polysciences; cacodylic acid, PIPES [piperazine-*N*,*N*′-bis(2-ethanesulfonic acid)], methylcellulose, polyvinylpyrrolidone, and 4,6-diamidino-2-phenylindole (DAPI) were purchased from Sigma Chemical Company; Dulbecco's phosphate-buffered saline (PBS) and fetal bovine serum (FBS) were purchased from Irvine Scientific; and RPMI 1640 with L-glutamine and HEPES buffer were purchased from Cellgro. Chocolate agar plates enriched with hemoglobin and IsoVitale X were purchased from Becton Dickinson Microbiology Systems. DAMP [3-(2,4-dinitroanalino)-3′-amino-*N*-methyldipropylamine] was purchased from Oxford Biomedical Research. Texas Red-conjugated human transferrin, LysoTracker red DND-99, and Prolong antifade mounting medium were purchased from Molecular Probes.

A rabbit polyclonal antibody to *F. tularensis* was purchased from Becton Dickinson. Mouse monoclonal antibodies to the following antigens were purchased from the indicated sources: *F. tularensis* lipopolysaccharide, Serotec; transferrin receptor and CD63 (lysosomal integral membrane protein), AMAC; human LAMP-1 (clone H4A3) and LAMP-2 (clone H4B4), University of Iowa Hybridoma Bank; early endosomal antigen 1 (EEA1), Transduction Laboratories; and cathepsin D, CIBA-Corning Diagnostics. Oregon Green-conjugated goat anti-mouse immunoglobulin G (IgG), Texas Red-conjugated goat anti-rabbit IgG, and Alexa fluor 350-conjugated goat anti-mouse IgG were purchased from Molecular Probes. Protein A-colloidal gold conjugates (5-, 10-, and 15-nm diameters) were provided by G. Posthuma (Utrecht University, Utrecht, The Netherlands). Goat anti-mouse IgG– and goat anti-rabbit IgG–colloidal gold conjugates were purchased from Sigma Chemical Company. All antisera other than those conjugated to colloidal gold were cleared of aggregates by ultracentrifugation (100,000 × *g* for 1 h) and filtration (with a 0.2-μm-pore-size filter) prior to use. All colloidal gold conjugates were filtered through a 0.2-μm-pore-size filter immediately prior to use.

Bacteria. The *F. tularensis* LVS, *F. tularensis* subsp. *holarctica* (type B), and a virulent RCI of *F. tularensis* subsp. *tularensis* (type A) (NY 96-3369) were obtained from the Centers for Disease Control and Prevention (Atlanta, Ga.). The bacteria were passaged through monolayers of macrophage-like THP-1 cells and stored frozen at −85°C. Before each infection experiment, the bacteria were thawed, grown for 1 day on chocolate agar plates enriched with IsoVitale X and hemoglobin, and suspended in normal saline. The concentration of organisms was determined by measurement of the optical density at 540 nm and by counting in a Petroff-Hausser chamber, and the bacterial suspension was diluted with RPMI 1640 containing fresh 10% autologous or AB serum to the desired multiplicity of infection. The viability of the bacteria was determined by plating serial dilutions of the infecting inoculum on enriched chocolate agar and by fluorescence microscopy with a Molecular Probes Dead-Live kit (Sytox-9 and propidium iodide) used according to the manufacturer's instructions. The viability was consistently higher than 99%. Work with virulent *F. tularensis* was conducted in a biosafety level 3 facility and was approved by the UCLA Institutional Biosafety Committee.

We prepared formalin-killed bacteria by suspending the bacteria in 4% paraformaldehyde in PBS overnight, washing the bacteria with PBS, quenching residual aldehydes with 10 mM glycine in PBS, and washing the bacteria an additional three times in PBS by centrifugation.

Human peripheral blood mononuclear cells. Heparinized blood from healthy human blood donors was diluted 1:1 with 0.9% saline, and the mononuclear cell fraction was obtained by centrifugation at 800 × *g* for 30 min at 24°C over a Ficoll-sodium diatrizoate solution (Ficoll-Paque; Pharmacia Fine Chemicals, Inc.). The layer containing the mononuclear cell fraction was removed and diluted 1:1 with RPMI 1640, and the mononuclear cells were collected by centrifugation at 400 × *g* for 10 min at 4°C. The mononuclear cells were washed twice by centrifugation at 115 × *g* for 10 min at 4°C, resuspended in RPMI 1640, counted in a hemocytometer (Clay Adams Division, Becton Dickinson and Co.), and adjusted to a concentration of 3×10^6 cells/ml in RPMI 1640 containing 20% autologous serum. The monocytes were allowed to differentiate into macrophages by incubation for 5 days at 37°C in 5% CO_2, either in sterile screw-cap Teflon wells or adhered to 75-cm^2 plastic tissue culture flasks (Costar), prior to use in infection experiments. Cells that were incubated for 5 days in Teflon wells were resuspended in ice-cold RPMI 1640 with 10% autologous serum and plated on glass or plastic (Wako Pure Chemical Industries, Ltd., Osaka, Japan) coverslips in 2-cm^2 tissue culture wells (1.5×10^6 cells/coverslip in 0.5 to 1 ml of culture medium). Cells were allowed to adhere to the coverslips or tissue culture plates for 90 min at 37°C in 5% CO_2, washed twice with RPMI 1640, and incubated overnight in fresh culture medium with 10% autologous serum prior to use in infection experiments. The participation of healthy human blood donors in our research was approved by the UCLA Institutional Review Board.

THP-1 cells. THP-1 cells (TIB 202; American Type Culture Collection) were added to glass or plastic coverslips in 2-cm^2 tissue culture wells or 75-cm^2 plastic tissue culture plates (1.5×10^5 cells/cm^2) and differentiated with phorbol myristate acetate (PMA; 100 nM) in RPMI 1640 with 10% heat-inactivated FBS (HI-FBS) for 3 days at 37°C in air containing 5% CO_2 prior to use in infection experiments.

Examination of growth of *F. tularensis* in macrophage monolayers. Monolayers of PMA-differentiated THP-1 cells on glass coverslips, prepared as described above, were incubated for 60 min with the attenuated LVS of *F. tularensis* or with the virulent RCI at a multiplicity of infection (MOI) of 35:1 (bacteria to monocytes) in RPMI containing 10% fresh AB serum. Nonadherent bacteria were removed by three washes, and the monolayers were incubated in RPMI containing 10% HI-FBS, fixed and permeabilized with acetone (−20°C), and immunostained for *F. tularensis* as described below at sequential times 0 to 8 h after infection. Randomly selected areas of the coverslips were examined by confocal

immunofluorescence microscopy, and the numbers of bacteria per monocyte were determined.

The percentage of bacteria that were adherent but not internalized was determined by fixing of the bacteria in 4% paraformaldehyde in PBS for 10 min, washing with PBS, immunostaining with a mouse monoclonal antibody to *F. tularensis* LPS, washing with PBS, permeabilizing with 0.1% Triton X-100, incubating with a rabbit anti-*F. tularensis* antibody, subsequently incubating with Oregon Green-conjugated goat anti-mouse and Texas Red-conjugated goat anti-rabbit antibodies, washing, mounting, and viewing as described below.

Immunofluorescence microscopy. Monolayers of differentiated THP-1 cells or human monocytes on coverslips were incubated for 60 to 90 min with the *F. tularensis* LVS or RCI at an MOI of 35:1 in RPMI 1640 containing 10% fresh AB serum (THP-1 cells) or autologous serum (monocytes) and 10% HI-FBS. Monolayers were washed with the culture medium, incubated in fresh medium at 37°C for an additional 0 to 14 h, fixed and permeabilized in methanol or acetone at −20°C, air dried, and incubated with 5% goat serum in PBS with 1% bovine serum albumin (BSA) to block nonspecific staining. Coverslips were stained simultaneously with the rabbit and mouse primary antibodies diluted in the same buffer overnight at 4°C. The anti-*F. tularensis* antibody was used at a dilution of 1:2,000 and the mouse monoclonal antibodies and isotypic control monoclonal antibodies (as negative controls) were used at a concentration of 5 μg/ml. Coverslips were washed with PBS and incubated with secondary antibodies (Oregon Green-conjugated goat anti-mouse IgG and Texas Red-conjugated goat anti-rabbit IgG, both diluted 1:50 in 5% goat serum–1% BSA in PBS) for 90 min at room temperature. The bacteria on the coverslips were washed in PBS, postfixed in 2% paraformaldehyde in PBS, incubated with 2.5 μM DAPI in PBS for 15 min at room temperature, washed with water, blotted, and mounted with Prolong antifade mounting medium, and images were acquired with a Leica TCS-SP confocal and two-photon microscope and Leica confocal software. Texas Red, Oregon Green, and DAPI fluorescence images were acquired sequentially by confocal scanning microscopy with confocal krypton and argon lasers and by two-photon scanning with a short-pulsed titanium-sapphire laser, respectively.

Texas Red-transferrin labeling of early endosomes. The extent to which the *F. tularensis* vacuole can acquire transferrin from early endosomes was assessed by infecting monolayers of human monocytes with the *F. tularensis* RCI or LVS as described above, washing the cells three times with serum-free medium (RPMI 1640 containing 20 mM HEPES, pH 7.4) to remove unlabeled transferrin, incubating the monolayers in serum-free culture medium containing 0.05 mg of Texas Red-conjugated transferrin/ml and 0.1% human serum albumin for 1 to 2 h at 37°C, fixing the cells, and staining for immunofluorescence as described above.

Interaction of *F. tularensis* compartment with EEA1 at early times after infection. To examine the early events after the uptake of *F. tularensis*, we synchronized the uptake of bacteria by macrophages. We preopsonized live or formalin-killed *F. tularensis* bacteria by incubation with 20% autologous serum (human MDM) or AB serum (THP-1 cells) in RPMI at 37°C for 30 min, chilled the bacterial suspension to 0°C, and adhered the opsonized bacteria to monolayers of macrophages on coverslips by incubating them at 0°C for 30 min. The monolayers were washed three times with ice-cold culture medium, and then the final wash medium was replaced with prewarmed (37°C) RPMI containing 10% HI-FBS to allow the macrophages to internalize the bacteria. After incubation for 5, 10, 15, 30, or 60 min at 37°C, the monolayers were fixed for 30 min in 4% paraformaldehyde in phosphate buffer, permeabilized with 0.1% Triton X-100, stained for immunofluorescence of EEA1 with a mouse monoclonal antibody (or an IgG1 isotypic control mouse monoclonal antibody) and Oregon Green-conjugated goat anti-mouse IgG, and stained for *F. tularensis* with a rabbit antibody and Texas Red-conjugated goat anti-rabbit IgG. The monolayers were stained with DAPI and then mounted, and fluorescence was evaluated by confocal microscopy as described above.

Labeling of acidified compartments with LysoTracker red DND-99. Monolayers of THP-1 cells or MDM were incubated with live or dead *F. tularensis* LVS or RCI as described above, washed, and incubated with 50 nM LysoTracker red DND-99 (34, 51) in RPMI containing 10% serum for 3 h at 37°C. Monolayers were fixed in 4% paraformaldehyde in PBS. Monolayers were stained with DAPI, washed, mounted, and viewed by laser scanning confocal and two-photon fluorescence microscopy as described above.

Assessment of intracellular pH by DAMP-immunogold staining. Human MDM or THP-1 cells were plated on plastic coverslips, incubated for 60 min with live or dead *F. tularensis* organisms, washed, and incubated in RPMI containing 10% HI-FBS as described above. After 2.5 h of incubation at 37°C, the culture medium was replaced with medium containing 30 μM DAMP (1, 38), and the monolayers were incubated for an additional 30 min at 37°C and fixed in a solution containing 2% paraformaldehyde, 0.5% glutaraldehyde in 0.1 M PIPES, pH 7.4, and 6% sucrose for 2 h at room temperature. The monolayers were dehydrated with a graded series of ethanol and embedded in LR White resin, and thin sections were collected on Formvar-coated nickel grids. Nonspecific antibody sites on the thin sections were blocked by incubating the grids for 30 min at room temperature on drops containing 1% BSA, 0.1% fish skin gelatin in 50 mM HEPES buffer, pH 7.4, 0.3 M NaCl, and 0.05% sodium azide (blocking buffer). The thin sections were stained for DAMP and *F. tularensis* by the sequential immunogold method (47), using a rabbit anti-dinitrophenol antibody (diluted 1:10,000) followed by 15-nm-diameter protein A-conjugated gold beads. Free protein A and Fc sites were destroyed by incubating the sections with 2% glutaraldehyde for 10 min. Aldehydes were quenched with 10 mM glycine in wash buffer, and the sections were incubated with a rabbit anti-*F. tularensis* antibody (diluted 1:10,000) and 5-nm-diameter protein A-conjugated gold beads. The sections were washed, postfixed in 2% glutaraldehyde, stained with uranyl acetate and lead citrate, and viewed with a JEOL 100 CX II electron microscope. Consecutive bacterial compartments were photomicrographed, and numbers of gold particles per unit area were calculated with a Numonics 2210 digitizer tablet and SigmaScan software (Jandel Scientific Co.). Estimations of the pHs of the intracellular compartments were performed as described by Orci et al. (38). This method depends upon the assumptions that DAMP accumulation is directly proportional to proton concentration, that aldehyde fixation retains DAMP in direct proportion to its concentration in the intracellular compartment, and that anti-dinitrophenol immunogold staining is directly proportional to the DAMP concentration in the compartment. With these assumptions, the pH of an intracellular compartment is given by the formula $pH = 7.0 - \log(D/N)$, where D is the concentration of gold particles per unit area over the unknown compartment and N is the concentration of gold particles per unit area over a compartment of neutral pH (the nucleus).

Cryoimmunoelectron microscopy. Monolayers of infected cells were fixed and prepared for cryoimmunoelectron microscopy according to our previously published procedures (13, 14). Infected cell monolayers were fixed in a mixture containing 4% paraformaldehyde, 0.1 M PIPES (pH 7.3), and 6% sucrose for 2 h at room temperature, washed with PBS, scraped with Costar cell scrapers into PBS containing 0.1% BSA, pelleted by centrifugation at 300 × *g* for 10 min at 4°C, resuspended in 10% gelatin (37°C), pelleted by centrifugation at 300 × *g* for 10 min at 37°C, solidified at 0°C, trimmed into 0.5-mm cubes, and cryoprotected in 2.3 M sucrose–20% polyvinylpyrrolidone in 0.1 M sodium phosphate, pH 7.0, overnight at 4°C. Gelatin-embedded, cryoprotected cells were frozen rapidly in liquid nitrogen, and thin sections were obtained at −90°C by using a Reichert Ultracut S ultramicrotome with an FCS cryoattachment. Thin sections were collected on drops of sucrose and methylcellulose and transferred to Formvar-coated nickel grids, and nonspecific sites were blocked with a solution containing 1% BSA, 0.1% fish skin gelatin in 0.05 M HEPES, pH 7.5, and 0.3 M NaCl (blocking buffer) for 1 h at 4°C. Immunogold double labeling and triple labeling were performed as described previously (13, 14), with a modification of the sequential protein A-gold technique described by Slot et al. (47). After the completion of double or triple immunogold labeling, sections were stabilized by incubation with 2% glutaraldehyde (10 min at 22°C), washed with distilled water, and embedded in 1.8% methylcellulose–0.4% uranyl acetate (26). Grids were examined by electron microscopy, and immunogold staining was quantitated as described above.

Fixation, staining, and Epon embedding for ultrastructural analysis. Monolayers of human MDM or THP-1 cells were incubated with the *F. tularensis* LVS or RCI at MOIs (bacteria to monocytes) of 500:1, 200:1, and 50:1 in RPMI 1640 containing 10% AB serum for 1 h at 37°C, washed, and fixed immediately (MOI of 500:1) or after an additional incubation for 3 h (MOI of 500:1), 6 h (MOI of 200:1), or 14 h (MOI of 50:1) at 37°C in RPMI 1640 containing 10% HI-FBS. (Relatively high MOIs were used to ensure that sufficient numbers of bacteria were available for electron microscopic ultrastructural analysis.) The monolayers were fixed in a combination of 2.5% glutaraldehyde and 1% osmium tetroxide in 0.1 M sodium cacodylate, pH 7.3, for 1 h at 0°C and were stained with 0.25% uranyl acetate in 0.1 M sodium acetate, pH 6.3, according to previously published procedures (28, 29). The monolayers were washed with ice-cold normal saline, scraped into normal saline with Costar cell scrapers, pelleted by centrifugation, embedded in 2% agarose in normal saline, dehydrated through a graded series of alcohol and propylene oxide, infiltrated sequentially with 2:1 and 1:1 propylene oxide-Epon for 4 h each, infiltrated overnight with 100% Epon, transferred to fresh Epon in embedding capsules, and polymerized at 60°C for 24 h. Thin sections were collected on Formvar-coated copper grids, stained with uranyl acetate and lead citrate, and viewed by electron microscopy as described above.

RESULTS

Growth of *F. tularensis* LVS and RCI in monolayers of human THP-1 cells. We examined the growth of the *F. tularensis* LVS, *F. tularensis* subsp. *holarctica*, and a virulent RCI of *F. tularensis* subsp. *tularensis* in monolayers of PMA-differentiated human macrophage-like THP-1 cell monolayers by enumerating the numbers of bacteria per monocyte by confocal immunofluorescence microscopy. After incubating THP-1 cells for 60 min with *F. tularensis* at an MOI of 35 bacteria to 1 THP-1 cell, we observed that 90% of the macrophages were infected, with an average of approximately 3 bacteria per monocyte. In the absence of permeabilization of the monolayer, approximately 88% of the bacteria were inaccessible to immunofluorescence staining, indicating that only 12% of the bacteria were external or incompletely internalized. With an additional incubation of the monolayers for up to 8 h before fixation and immunostaining, the numbers of both the *F. tularensis* RCI and the LVS increased exponentially in human THP-1 cells, with doubling times of 2.5 to 3 h (data not shown). We observed a similar exponential growth rate by lysing the monolayers 0 to 16 h after infection and determining the number of CFU per monolayer (data not shown).

Importantly, at the relatively low MOI employed, we obtained efficient uptake of the bacteria by THP-1 cells only when we used freshly prepared human AB serum that had been handled carefully to preserve complement (uptake of approximately three to four bacteria per THP-1 cell). The uptake of the bacteria was negligible (averaging <0.3 bacteria per THP-1 cell) when we used HI-FBS or human AB serum from either of two commercial sources (data not shown).

***F. tularensis* and early endosomal markers.** At early times after phagocytosis, phagosomes containing inert particles have the capacity to interact with and acquire the markers of early endosomes (21). Early endosomal markers include the transferrin receptor and its ligand, transferrin, and EEA1 (39, 46). We employed confocal immunofluorescence microscopy to examine the distribution of these markers in human MDM and THP-1 cells 1 to 4 h after infection with the *F. tularensis* RCI or LVS. When we examined monolayers of human MDM or THP-1 cells for these markers immediately after a 60-min incubation with the bacteria, we found that $<15\%$ of the internalized LVS or RCI bacteria exhibited any overlap in staining with these markers (data not shown). To examine earlier times, we preopsonized the bacteria and synchronized their uptake by allowing adherence at 0°C and then fixed the cells at sequential times after warming to 37°C. The EEA1 colocalization of both live and formalin-killed bacteria reached a maximum of 35 to 45% at 15 min, declining to 10 to 15% by 60 min. We found no difference in the kinetics or extent of EEA1 colocalization between the live and formalin-killed bacteria (Fig. 1).

Late endosomal/lysosomal markers transiently colocalize with *F. tularensis*. As they mature, phagosomes containing inert particles acquire an increasing capacity to interact with late endosomes and lysosomes and to acquire the markers of late endosomes and lysosomes (20, 21). These markers include CD63, a lysosomal integral membrane protein, LAMP-1, LAMP-2, and acid hydrolases such as cathepsin D. We employed confocal immunofluorescence microscopy to examine the distribution of CD63, LAMP-1, LAMP-2, and cathepsin D in human MDM and THP-1 cells at sequential times after infection. At early times after infection, we found an abundant colocalization of CD63, LAMP-1, and LAMP-2 with the *F. tularensis* LVS and RCI which reached a maximum of 60 to 70% 2 to 4 h after infection of the macrophages (Fig. 2 and 3). However, at times later than 4 h after infection, the colocalization of these markers with *F. tularensis* decreased to low levels, declining to 15% or less by 16 h after the infection in THP-1 cells (Fig. 2 and 3). We observed a similar transient localization of CD63 and LAMP-1 with the *F. tularensis* LVS and RCI in human MDM, with high initial levels of colocalization at times prior to 4 h of infection and a progressive loss of colocalization 8 to 14 h after infection (Fig. 2 and 3). Latex beads and formalin-killed *F. tularensis* colocalized extensively (70 to 100%) with CD63 and LAMP-1 at all time points in THP-1 cells (Fig. 2 and 3) and in MDM (data not shown). In all experiments, both with THP-1 cells and with MDM, we observed a more rapid decline in the colocalization of CD63 and LAMP-1 with the RCI than with the LVS. However, this trend did not reach statistical significance.

We also employed immunoelectron microscopy to examine the distribution of CD63 in cryosections of MDM infected with the *F. tularensis* RCI and LVS and confirmed that CD63 was relatively abundant on *F. tularensis* phagosomes 4 h after infection (Fig. 4A and 5 [top]). In contrast, we found that cathepsin D did not colocalize with the bacteria at this time point (Fig. 4B and 5 [bottom]). Latex bead phagosomes stained positively for both CD63 and cathepsin D at these time points (Fig. 4 and 5). Consistent with the confocal immunofluorescence microscopy results, the amount of CD63 staining associated with the *F. tularensis* bacteria in human MDM 8 h after infection was markedly reduced (data not shown).

Live, but not formalin-killed, *F. tularensis* organisms avoid residence in acidified compartments. LysoTracker red DND-99 is a lysosomotropic agent that is concentrated in acidified compartments when it is added to living cells and whose distribution within cells can be assessed by fluorescence microscopy after aldehyde fixation (34, 51). We employed this dye to determine whether live or dead *F. tularensis* bacteria enter acidified compartments in THP-1 cells 3 h after infection. We found that whereas heat-killed *F. tularensis* cells stained extensively for LysoTracker red DND-99, live *F. tularensis* RCI and LVS organisms only rarely colocalized with this marker (data not shown). These data indicate that live *F. tularensis* phagosomes do not reside in highly acidified vacuoles, whereas killed *F. tularensis* bacteria enter acidified phagolysosomes.

DAMP is a lysosomotropic agent that, when added to living cells, is concentrated in acidified compartments (1, 38). The molecule can be fixed in place by aldehyde fixatives, and its distribution can be determined and quantified by immunoelectron microscopy of resin-embedded thin sections. Quantitation of the numbers of DAMP-immunogold particles in the phagosomes and in a neutral reference compartment (the nucleus) allows a determination of the pH of the phagosome by a formula derived by Orci et al. (38).

We infected human MDM with the formalin-killed or live *F. tularensis* RCI, added DAMP to label the acidic compartments, and fixed and processed the monolayers for immunoelectron microscopy 3 h later. Whereas killed bacteria resided

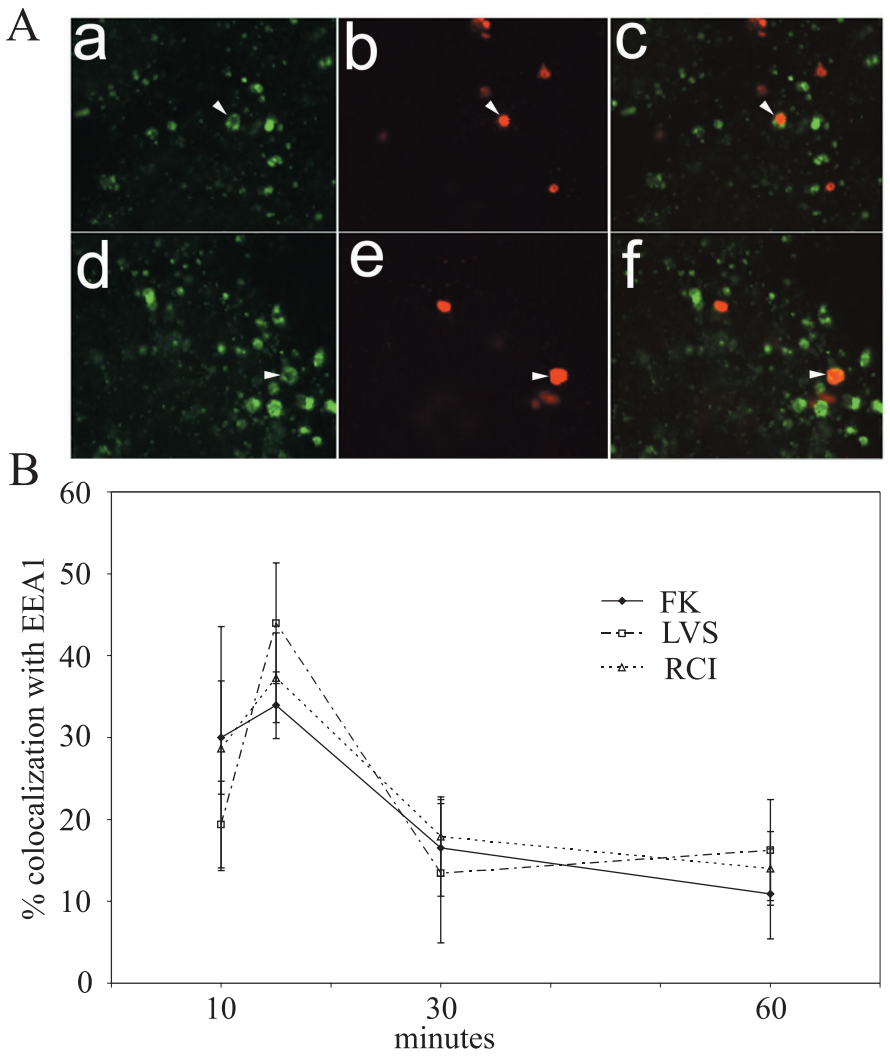

FIG. 1. Live and formalin-killed *F. tularensis* bacteria exhibit similar kinetics of colocalization with the early endosomal marker EEA1. (A) Preopsonized formalin-killed (a to c) or live *F. tularensis* RCI (d and e) was incubated with THP-1 cells at 0°C to allow adherence, but not uptake, washed, warmed to 37°C to allow for internalization, fixed after 10 to 60 min, and stained by immunofluorescence for EEA1 (green) (a and d) and for *F. tularensis* antigen (red) (b and e). Panels c and f show the merged green and red images. The panels show THP-1 cells fixed after 15 min. Arrows indicate bacteria that colocalized with EEA1. (B) Percentages of live (RCI or LVS) or formalin-killed (FK) *F. tularensis* RCI bacteria colocalizing with EEA1. The data represent the means ± standard errors. The experiment was performed three times, with similar results.

in DAMP-positive acidified compartments, the live *F. tularensis* RCI had relatively little colocalization with DAMP (Fig. 6). We calculated that the killed bacteria resided in phagosomes with a pH of 5.5, whereas live *F. tularensis* resided in a compartment with a pH of 6.7 (Fig. 7).

***F. tularensis* RCI and LVS reside in compartments with ultrastructurally distinct phagosomal membranes at early times after infection, but not at late times after infection, and many of the phagosomes are surrounded by a fibrillar coat.** We examined the ultrastructural appearance of *F. tularensis* in human THP-1 cells infected with the *F. tularensis* RCI and LVS at sequential times after infection. Immediately after infection, the majority of LVS and RCI bacteria resided within vacuoles with well-delineated membranes (Fig. 8 and 9). Approximately half of the phagosomal membranes were coated on their cytoplasmic sides with densely staining short filaments that extended 25 to 34 nm perpendicularly from the outer leaflet of the phagosomal membrane (Fig. 8). This fibrillar coating resembled clathrin-coated buds on the plasma membrane, except that the fibrillar phagosomal coats appeared to be more coarse, stained more intensely, and usually coated the entire circumference of the cytoplasmic aspect of the phagosomal membrane. These coated phagosomal membranes often appeared to be in the process of forming buds and vesicles and of fragmenting (Fig. 8). As a control, we examined the ultrastructure of formalin-killed *F. tularensis* bacteria in human MDM and found that these resided exclusively within membrane-bound compartments, with no evidence of fibrillar coats (data not shown). We also have not observed this phenomenon of fibrillar coats in ultrastructural analyses of *M. tuberculosis*, *Legionella pneumophila*, or *Escherichia coli* phagosomes in human MDM.

We previously described the recruitment of the endoplasmic reticulum, ribosomes, and mitochondria to the phagosomes of

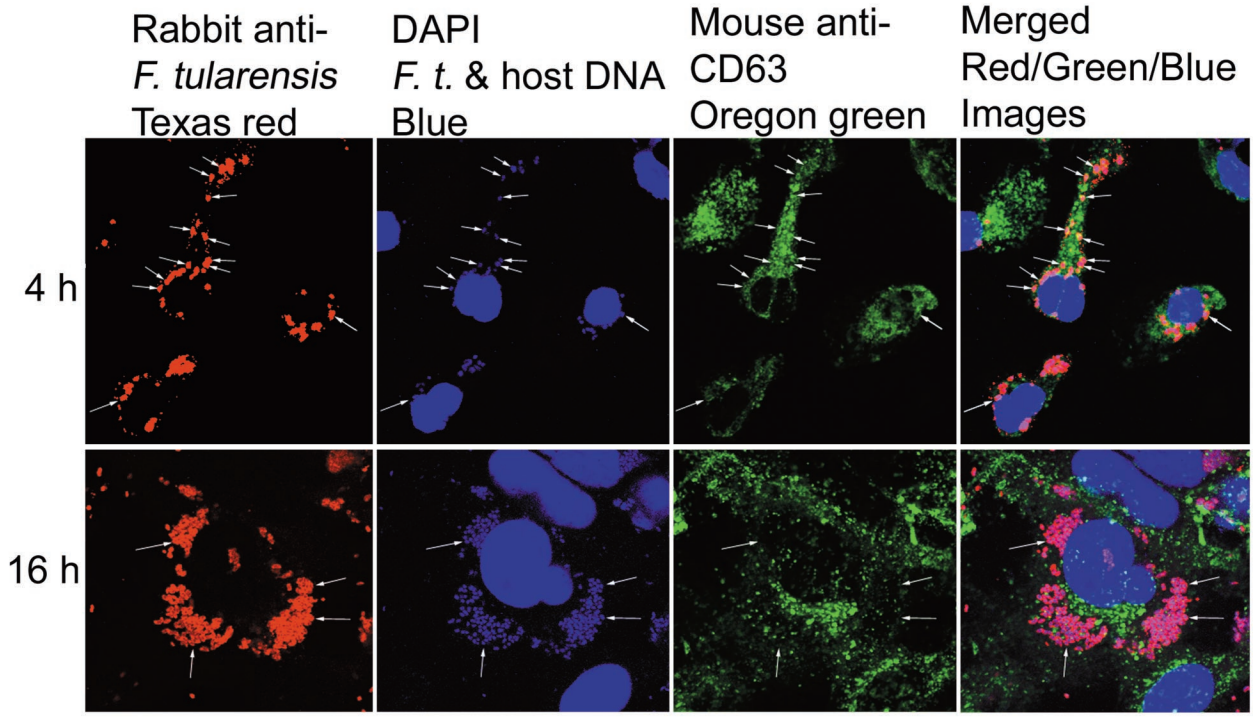

FIG. 2. Virulent RCI of *F. tularensis* colocalizes extensively with LAMP CD63 at 4 h but very little at 16 h after uptake by human THP-1 cells. THP-1 cells were infected with the RCI of *F. tularensis*, fixed 4 or 16 h after infection, stained for CD63 (Oregon Green), *F. tularensis* (Texas Red), and DNA (DAPI), and imaged by laser scanning confocal and two-photon fluorescence microscopy. After 4 h (top row), the majority of *F. tularensis* bacteria resided in compartments with intense staining around the rim for CD63 (arrows). After 16 h (bottom row), the bacteria had multiplied extensively and no longer colocalized with CD63. This experiment was performed twice, with similar results.

virulent *Legionella pneumophila* phagosomes (29). We examined the ultrastructure of the *F. tularensis* phagosomes at sequential times after infection and found no evidence of a consistent recruitment of ribosomes or endoplasmic reticulum to the *F. tularensis* phagosomes. We observed mitochondria adjacent to some *F. tularensis* phagosomes (e.g., see Fig. 8D) in a fashion that was reminiscent of the *Legionella pneumophila* phagosome (29), but this occurred with only 10% of the *F. tularensis* phagosomes.

The number of bacteria surrounded by a membrane declined rapidly after infection. Immediately after a 90-min incubation of the *F. tularensis* LVS or RCI with monocytes (Fig. 8A and E), 80 to 90% of the LVS or RCI bacteria were surrounded over at least half of their circumference by a phagosomal membrane. By 6 h after infection, <50% of the bacteria were surrounded by a phagosomal membrane, and by 14 h, the number was <20% (Fig. 9). We did frequently observe fragments of the membrane and vesicles coated with densely staining fibrils in the vicinity of many bacteria that otherwise lacked identifiable membranes at the 3- to 6-h time points. Despite the absence of discernible membrane structures around the LVS or RCI bacteria at later time points, the bacteria were uniformly surrounded by an electron lucent zone that was about 0.3 μm wide. This electron lucent zone may have reflected a bacterial capsule which did not stain well by the osmium, lead, or uranyl acetate staining methods employed, or it may have reflected a shrinkage of the bacteria during dehydration and embedding. A similar lucent zone was observed for intracytoplasmic *Shigella flexneri* and was attrib-

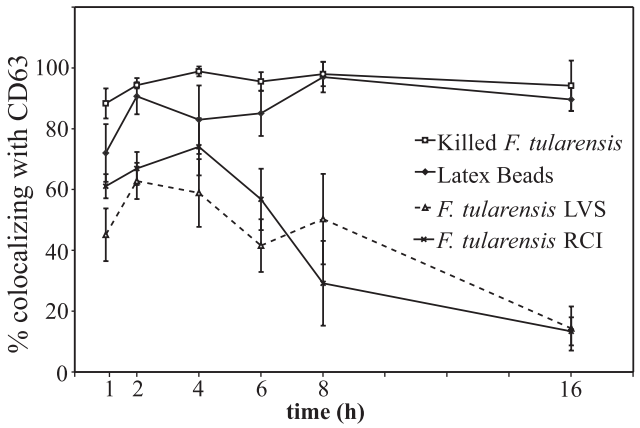

FIG. 3. Quantitation of immunofluorescence staining for CD63 in THP-1 cells infected with *F. tularensis* RCI or LVS. Monolayers of human THP-1 cells were incubated with latex beads, formalin-killed *F. tularensis*, or live *F. tularensis* LVS or RCI as described in the text. Monolayers were washed, incubated for an additional 1 to 16 h, fixed, permeabilized, stained for CD63 and *F. tularensis* by using immunofluorescence reagents, and examined by confocal and two-photon laser scanning fluorescence microscopy, and the numbers of bacteria and latex beads that colocalized with CD63 were enumerated. Colocalization of the *F. tularensis* RCI and LVS with CD63 reached a maximum of 60 to 70% 2 to 4 h after infection. Thereafter, with continued intracellular multiplication, the colocalization of *F. tularensis* with CD63 steadily declined, falling to 15% by 16 h. Latex beads and formalin-killed *F. tularensis* colocalized extensively (70 to 95%) with CD63 at all time points. This experiment was performed twice, with similar results. Similar results were also obtained with LAMP1 and LAMP2 and when MDM were used.

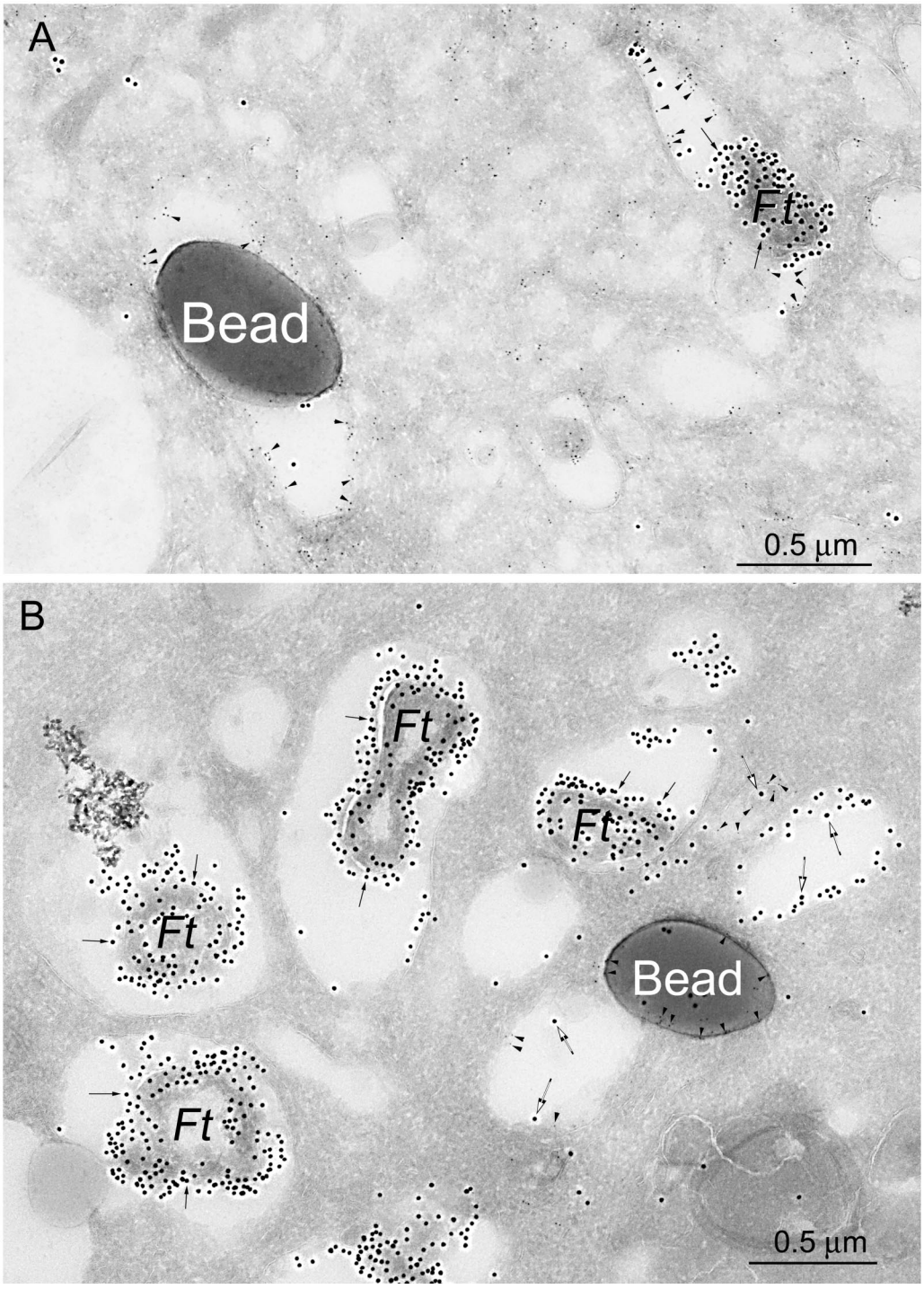

FIG. 4. Immunoelectron microscopy demonstrates that CD63, but not cathepsin D, is present on *F. tularensis* phagosomes, whereas both markers are present on latex bead phagosomes in human MDM 4 h after infection. Human monocytes were isolated from peripheral blood, differentiated for 5 days in Teflon wells, plated on tissue culture plastic, incubated with the *F. tularensis* RCI and latex beads as described in the text, and fixed and prepared for cryoimmunoelectron microscopy. (A) Sections were stained with immunogold for CD63 (5-nm-diameter immunogold; arrowheads) and *F. tularensis* (15-nm-diameter immunogold; arrows). Both the *F. tularensis* phagosome and the latex bead phagosome stained positively for CD63. (B) Sections were stained for cathepsin D (5-nm-diameter immunogold particles; arrowheads) and *F. tularensis* (15-nm-diameter immunogold particles; arrows). Whereas the latex bead phagosomes had abundant staining for cathepsin D, the bacterial phagosomes had no staining for cathepsin D. Some *F. tularensis* antigen (15-nm-diameter gold) was also present in compartments outside of the phagosomes (larger, open arrows).

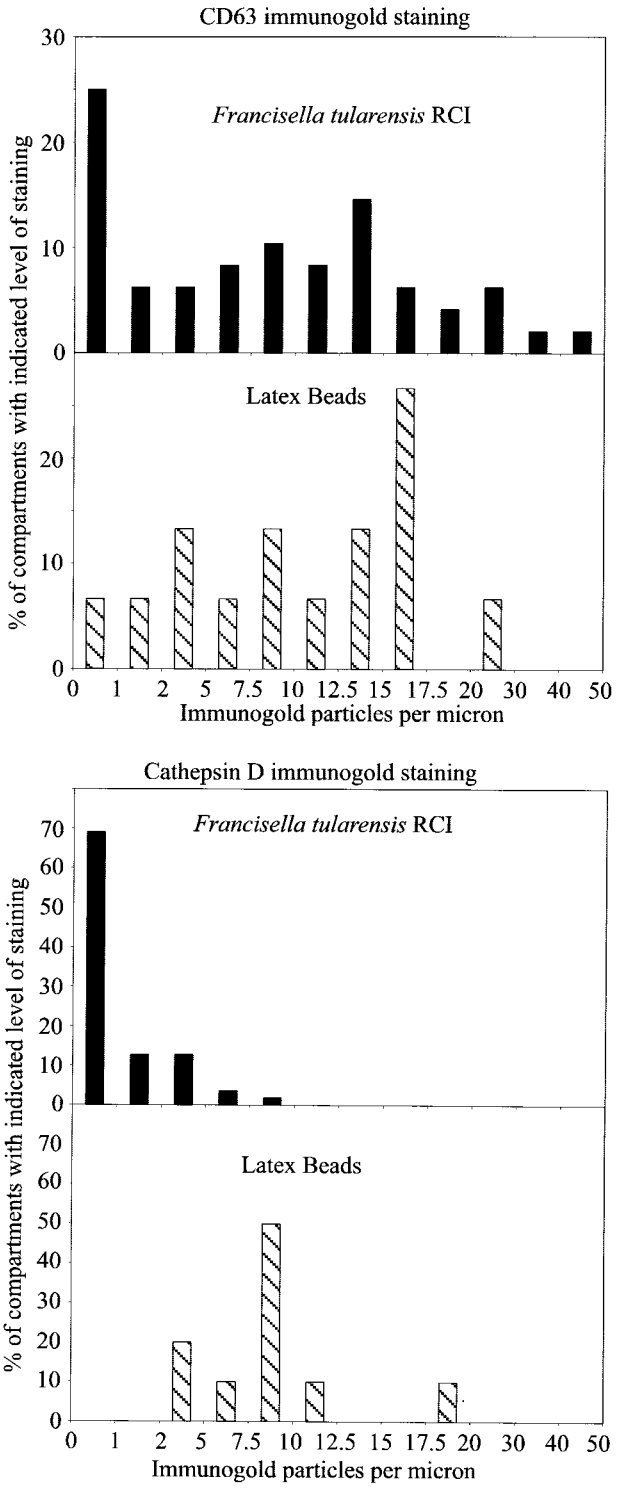

FIG. 5. Quantitation of immunogold staining of *F. tularensis* RCI phagosomes 4 h after infection of human MDM. Histograms demonstrate the distribution of immunogold staining for CD63 (top) and cathepsin D (bottom) in phagosomes fixed 4 h after coincubation with the *F. tularensis* RCI and latex beads. Whereas the majority of both *F. tularensis* phagosomes and latex bead phagosomes acquired abundant staining for CD63, only latex bead phagosomes showed abundant staining for cathepsin D. Control sections incubated with isotypic control mouse myeloma Igs had <0.25 gold particles per μm of membrane. The experiment was performed twice, with similar results.

uted to bacterial shrinkage during dehydration and embedding (42). The size of the lucent zone was diminished by the use of a freeze substitution embedding technique (42).

The loss of phagosomal membrane definition was not due to apoptosis, necrosis, or a deterioration in the ultrastructure of the infected cells. We assessed the overall viability and integrity of the infected monolayers by trypan blue exclusion. For the first 8 h after infection, >99% of the infected THP-1 cells excluded trypan blue. By 16 h after infection, 70% of the LVS-infected cells continued to exclude trypan blue and 50% of the RCI-infected cells excluded trypan blue. Ultrastructurally, we did observe substantial numbers of both necrotic cells and apoptotic cells 14 h or later after infection (as has been reported previously [33]). However, the loss of phagosomal membranes was observed for 10 to 20% of the bacteria 1 h after infection and for 50 to 60% of bacteria by 6 h after infection (Fig. 9). The loss of a phagosomal membrane occurs in lightly infected cells and in cells that have an excellent preservation of the membrane ultrastructure. Golovliov et al. (25) have also emphasized that a disruption of phagosomal membranes can be seen in cells that are lightly infected by the *F. tularensis* LVS.

DISCUSSION

Intracellular parasites have been shown to subvert the host cell's normal membrane trafficking pathways to achieve intracellular compartments that are more hospitable to their growth and multiplication. Even within the three general pathways of intracellular parasites, namely the extraphagosomal pathway, by which the pathogen resides freely within the cytoplasm, the phagolysosomal pathway, and the phagosomal pathway, by which the pathogen resides in a phagosome that does not fuse with lysosomes, there is considerable variation that makes each pathogen's pathway unique. Understanding the unique membrane trafficking patterns of intracellular parasites can shed light on the pathogenic mechanisms that these parasites employ to subvert host cell defenses. Relatively few studies have examined the intracellular compartment of *F. tularensis* or the interactions between the *F. tularensis* compartment and the host cell, and they have examined only the attenuated *F. tularensis* LVS (subsp. *holarctica*). Anthony et al. (2) examined mouse macrophages infected with the *F. tularensis* LVS at 4 to 7 h postinfection and observed vacuoles containing one or more bacteria. Bacteria were not observed free in the cytoplasm and the bacterial phagosomes were observed not to fuse with lysosomes that had been prelabeled with colloidal thorium. The presence or absence of particular molecular membrane markers on the *F. tularensis* LVS phagosome was not examined in the study of Anthony et al. (2). Golovliov et al. (25) recently reported that the majority of *F. tularensis* LVS organisms colocalized with LAMP-1 immunofluorescence staining within the first hour after infection and declined to a 30% level of colocalization by 3 h after infection. These authors also observed that >90% of the LVS bacteria escaped into the cytoplasm of infected mouse macrophages and human THP-1 cells. The apparent escape of *F. tularensis* Schu S4 bacteria into the cytoplasm has also been described in an in vivo study of infected mouse tissues (32), but the number of such bacteria was not quantified, as infected tissues can be

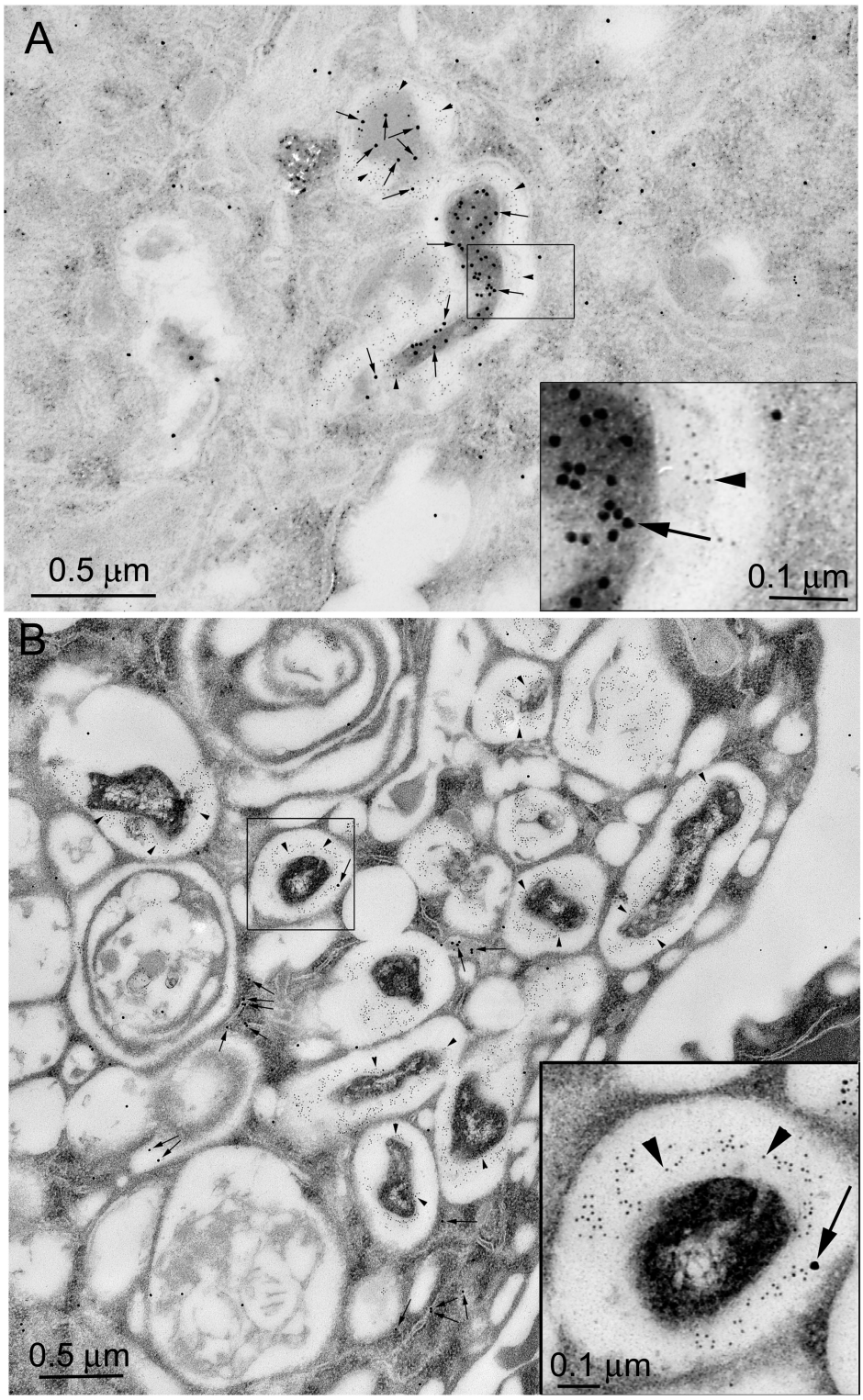

FIG. 6. Killed, but not live, *F. tularensis* RCI bacteria enter acidified compartments that stain positive for DAMP in human MDM. Human MDM were fixed 3 h after infection with formalin-killed (A) or live (B) *F. tularensis* RCI, and acidified compartments were identified by DAMP immunogold staining (15-nm-diameter gold particles; arrows) and immunoelectron microscopy as described in the text. *F. tularensis* antigen was identified by immunostaining with 5-nm-diameter gold particles (arrowheads). Abundant staining for DAMP was associated with killed *F. tularensis* (A) but not live *F. tularensis* (B). This experiment was performed twice, with similar results.

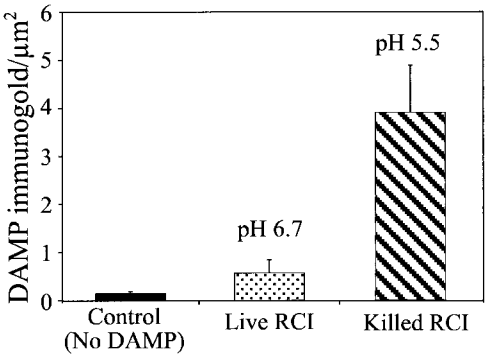

FIG. 7. Calculation of phagosomal pH by quantitative immunogold staining. Human MDM were infected with the live or killed *F. tularensis* RCI as described for Fig. 6, and DAMP immunogold particles were enumerated in the bacterial compartments and in a reference compartment (the nucleus). The pH was calculated as described in Materials and Methods. Values shown are the means ± standard errors of at least 20 bacterial compartments from each of at least two electron microscopy grids. The experiment was performed twice, with similar results.

technically difficult to fix and embed for ultrastructural analysis and quantitation. Prior to this study, ultrastructural studies and membrane trafficking studies of the interaction of virulent *F. tularensis* subsp. *tularensis* with human macrophages had not been published.

Anthony et al.'s (2) observation that the LVS bacteria do not fuse with thorium-labeled lysosomes appears to contradict our observations regarding the LVS and the RCI and those of Golovliov et al. regarding the LVS, i.e., that the bacteria do initially colocalize with LAMPs. However, we did not observe significant levels of cathepsin D associated with *F. tularensis*. It is possible that the bacterial phagosomes fuse with vesicles that contain LAMP-1 and CD63 but do not contain cathepsin D or endocytosed markers. Alternatively, even if the phagosomes do fuse with vesicles containing cathepsin D or endocytosed markers, it is possible that permeabilization or disruption of the phagosomal membrane promotes the diffusion of endocytosed markers and cathepsin D away from the bacteria. A higher degree of colocalization was obtained for the integral membrane proteins LAMP-1 and CD63 because membrane fragments bearing these markers remained in the vicinity of the bacteria.

The pHs of the compartments of several intracellular parasites have been measured. Pathogens such as *Leishmania amazonensis* (3) and *Coxiella burnetii* (27) reside in highly acidified phagolysosomes. Pathogens such as *Chlamydia trachomatis*, *Legionella pneumophila*, and *M. tuberculosis* have been demonstrated to reside in phagosomes that are only minimally acidified (18, 27, 31). In each of these cases, the pH of the intracellular compartment is consistent with the pH that has been shown to be favorable for the parasite's metabolic requirements or for its growth on a defined culture medium. The interactions with the host cell membrane trafficking machinery that result in a hospitable pH are an important aspect of an intracellular parasite's pathogenetic mechanisms. However, no reports describe a direct assessment of the pH of vacuoles containing either a fully virulent strain or the attenuated LVS of *F. tularensis*. We employed light and electron microscopy techniques to evaluate the pH of the *F. tularensis* compartment and found that it is not significantly acidified. This is consistent with the observation that *F. tularensis* grows best in broth culture at a neutral pH. Permeabilization or disruption of the phagosomal membrane would prevent acidification of the phagosome.

We observed a transient colocalization of approximately 40% of the LVS and RCI phagosomes with the early endosomal antigen EEA1 15 min after infection which declined to 15% by 60 min after infection. This pattern of colocalization with EEA1 did not differ from that observed for formalin-killed bacteria, supporting the hypothesis that important differences in membrane trafficking between dead and live *F. tularensis* phagosomes occur subsequent to EEA1 acquisition, i.e., after the limited acquisition of late endosomal markers.

Fortier et al. have reported that the growth of *F. tularensis* requires iron from the host cell and that the liberation of iron for utilization by this bacterium requires endosomal acidification (23). Blocking of acidification with the vacuolar proton pump inhibitor bafilomycin inhibited the intracellular growth of *F. tularensis*. While the authors interpreted this to mean that acidification of the *F. tularensis* phagosome is required for its growth, it should be noted that the acidification of early endosomes is required to liberate iron from transferrin and that the treatment of a eukaryotic cell with bafilomycin will limit the availability of iron to all compartments within the host cell. Ordinarily, iron remains bound to transferrin at a neutral pH but dissociates from transferrin at the early endosomal pH of 5.5 to 6. Thus, even in the case of a bacterium that resides freely in the cytoplasm, the inhibition of endosomal acidification would be expected to deprive the bacterium of essential iron. It is not known whether transferrin traffics directly to the *F. tularensis* compartment within infected cells or if *F. tularensis* instead receives its iron from other intracellular iron intermediates. We examined the trafficking of fluorescently labeled transferrin in human MDM infected with the *F. tularensis* LVS and RCI and did not observe an appreciable colocalization of transferrin with the bacteria 1 to 2 h after infection. However, since we did observe a transient colocalization of EEA1 with approximately 40% of the *F. tularensis* phagosomes 15 min after infection, it is likely that transferrin is also delivered to the early *F. tularensis* phagosome but that it is not easily detected at the 1- to 2-h time points that we examined.

We believe that the absence of identifiable phagosomal membranes by ultrastructural analysis of Epon resin-embedded sections at time points after 4 h reflects a true absence of the phagosomal membrane and the escape of the bacteria into the cytoplasm. A number of artifacts during processing for electron microscopy can lead to a failure to detect phagosomal membranes. Membrane definition can be lost in areas of the sample that are not well infiltrated by the resin, a problem that can occur in the vicinity of bacterial capsules. However, since the bacterial membranes were easily discernible at early times after infection, this is not an adequate explanation of the virtually complete absence of phagosomal membranes at later times after infection. Membranes that lack appreciable protein content are also not stained well by heavy-metal stains (lead, uranium, and osmium), and lipids may be extracted by the organic solvents (ethanol and propylene oxide) employed for dehydration and embedding. However, our observations that

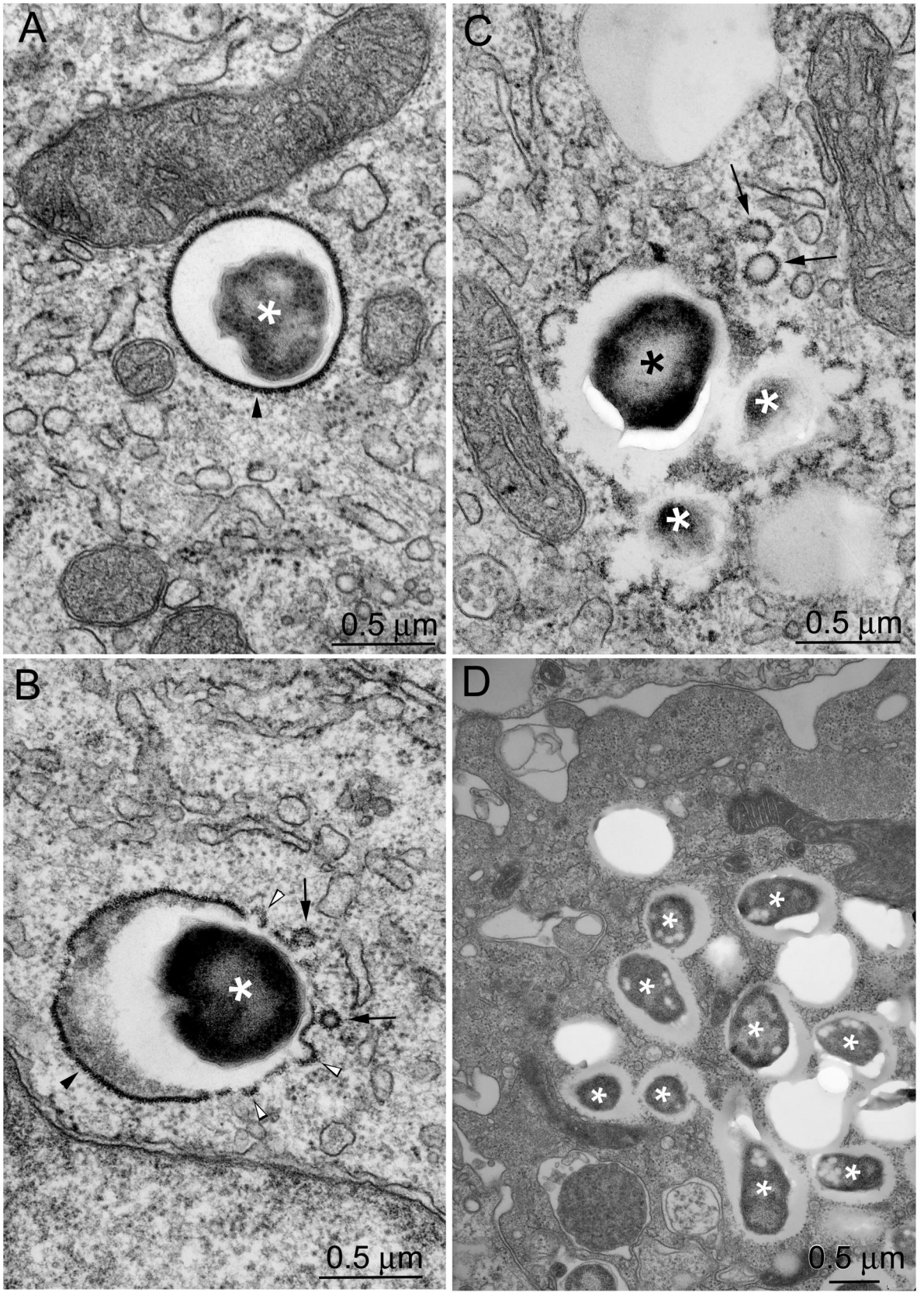
A
0.5 μm
C
0.5 μm
B
0.5 μm
D
0.5 μm

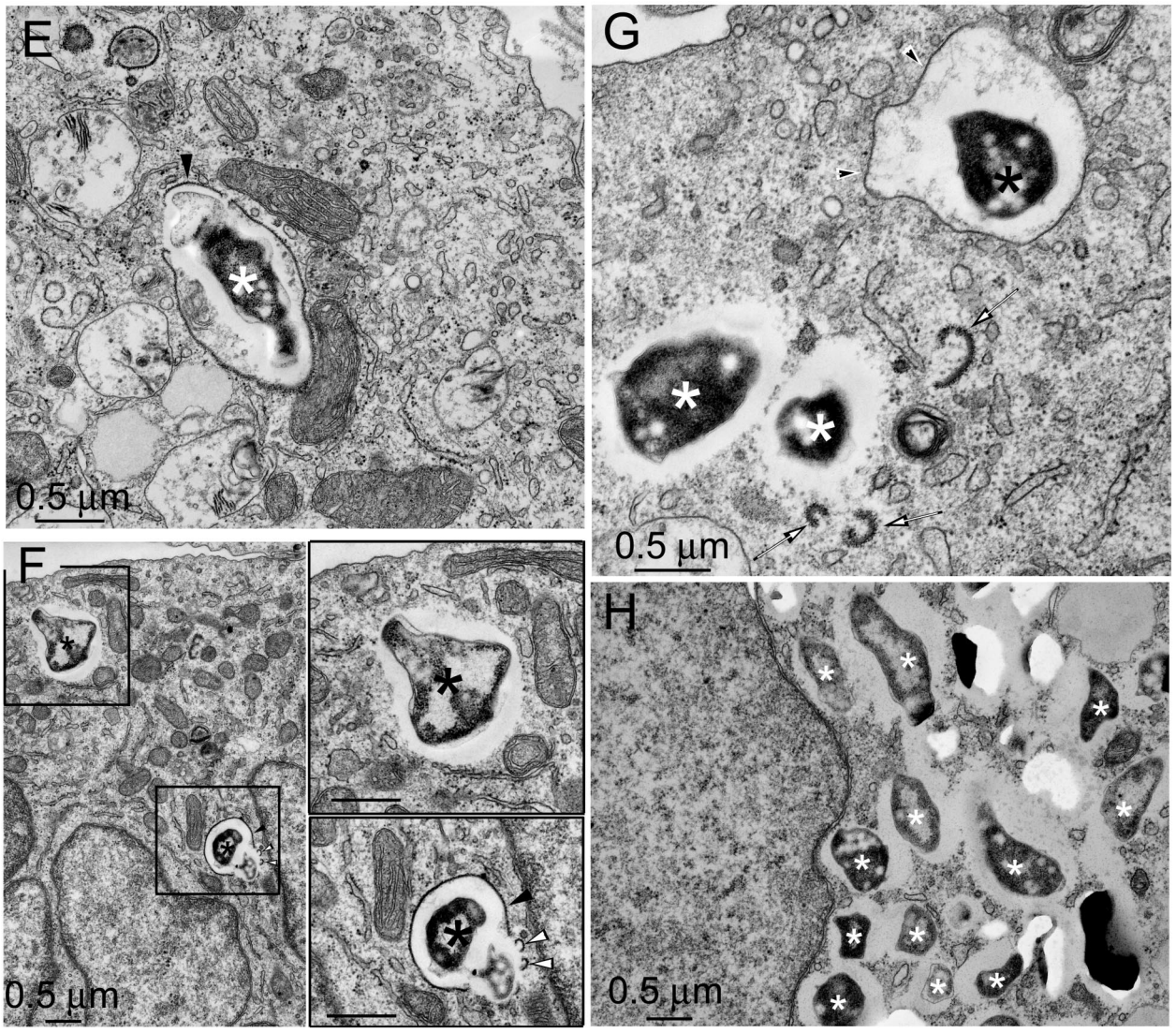

FIG. 8. *F. tularensis* LVS and RCI are within vacuoles with clearly discernible membranes at early times after infection, but not at late times after infection. THP-1 cells were incubated for 90 min with the *F. tularensis* LVS (A to D) or RCI (E to H) and fixed immediately (A and E) or after an additional 3 h (B and F), 6 h (C and G), or 14 h (D and H). Monolayers were fixed with osmium tetroxide and glutaraldehyde, stained with uranyl acetate, embedded in Epon resin, thin sectioned, enhanced for contrast with uranyl acetate and lead citrate, and viewed by electron microscopy. Host cell membranes were well preserved in all sections. Bacteria are indicated by asterisks. Immediately after infection, the majority of *F. tularensis* LVS (A) and RCI (E) bacteria resided in compartments with easily discernible phagosomal membranes. Many bacterial phagosomal membranes had a thick fibrillar coat radiating approximately 30 nm from the cytoplasmic aspect of the membrane (A, B, E, and F; solid arrowheads). In other cases, the phagosomal membranes lacked these coats (e.g., white arrowheads in panel G). The coated membranes appeared to form buds (B and F [lower insert], open arrowheads), to pinch off and form vesicles (B and C, solid arrows), or to fragment (G, open arrows). By 14 h after infection, the majority of LVS (D) and RCI (H) bacteria (asterisks) lacked any identifiable phagosomal membranes. In all cases, the bacteria were separated from the host cell cytoplasm by electron lucent zones. Bars, 0.5 μm. This experiment was performed twice, with similar results.

at early time points, many phagosomal membranes were densely coated on their cytoplasmic aspect with a fibrillar material, and that the membranes appeared to be undergoing a process of budding, vesiculation, and fragmentation make this explanation unlikely.

The mechanisms that allow the attenuated LVS and the virulent RCI of *F. tularensis* to deviate from the phagolysosomal pathway and to disrupt their phagosomal membrane are unclear. To date, no hemolysins, phospholipases, or porins have been reported for the genome of *F. tularensis* Schu. Golovliov et al. (25) reported observing vesicles of bacterial origin within the translucent zone adjacent to the bacteria and suggested that these glycolipid vesicles may be involved in permeabilizing the phagosomal membrane. We do frequently observe immunogold staining for *F. tularensis* antigens in the translucent zone and at the outer perimeter of the translucent zone both in our frozen sections and in LR White resin-embedded sections. In addition, both by immunogold staining and by immunofluorescence staining, we frequently observe a vesicular pattern of staining for *F. tularensis* antigen in the vicin-

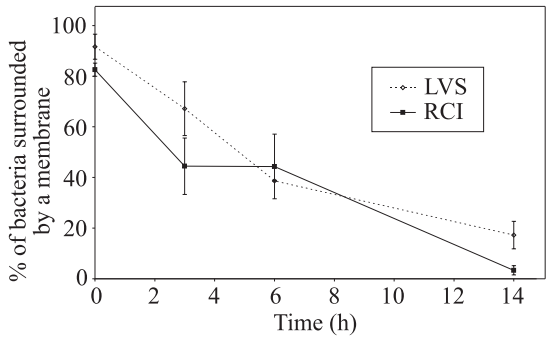

FIG. 9. Quantitation of bacteria surrounded by phagosomal membranes. THP-1 cells were infected with the *F. tularensis* LVS or RCI and prepared for transmission electron microscopy as described in the text. Bacteria were scored as having a phagosomal membrane if at least 50% of their circumference was surrounded by a morphologically discrete membrane bilayer. Eighty to 90% of the bacteria had identifiable membrane bilayers when they were fixed immediately after a 90-min incubation with THP-1 cells (0 h); the percentage dropped to <20% by 14 h after infection. In the first 6 h after infection, 40 to 50% of the RCI phagosomes and 58 to 88% of the LVS phagosomes had densely staining fibrillar coats (data not shown). At 14 h, it was difficult to quantify the fraction of phagosomes with fibrillar coats because very few phagosomal membranes were visible. This experiment was performed twice, with similar results.

ity of, but outside of, the *F. tularensis* phagosome. These vesicles containing *F. tularensis* antigen frequently have lysosomal markers, such as CD63 and cathepsin D, as well. However, we do not observe immunogold staining for *F. tularensis* antigens on the cytoplasmic aspect of the phagosomes or on the cytoplasmic perimeter of the lucent zones. While it is possible that the fibrillar coat material could be a bacterial product that is not recognized by our rabbit polyclonal anti-*F. tularensis* antiserum, we suspect that these dense fibrillar coats are of a host rather than bacterial origin. The bacteria may trigger a host process similar to that involved in the formation of clathrin-coated vesicles that instead leads to disruption of the phagosome. Further experiments are under way to determine the identity of the phagosomal coat material. The mechanisms that allow *F. tularensis* to deviate from the classic phagolysosomal pathway and to disrupt its phagosomal membrane are likely to be of critical importance to the virulence of the bacterium.

None of the analyses employed in this study revealed major differences between the virulent and vaccine strains. It is likely that additional factors apart from those that we have studied here are critical for *F. tularensis* virulence. Important aspects of pathogenicity that this study has not addressed include (i) the efficiency of cell-to-cell spread of bacteria at late stages of infection, (ii) the relative cytotoxicity of bacteria at late stages of infection, and (iii) the capacities of different strains to induce an effective versus a maladaptive immune response.

Our observation that the uptake of *F. tularensis* by human macrophages requires serum prepared in a fashion that preserves complement activity suggests that uptake may be promoted by complement receptors interacting with complement fixed on the surfaces of the bacteria. Complement and/or complement receptors have been shown to play a role in the internalization of many other intracellular pathogens, including *Legionella pneumophila* (40), *M. tuberculosis* (45), *Mycobacterium leprae* (43, 44), *Mycobacterium avium* (6), *Leishmania donovani* (7), *Leishmania major* (36), *Listeria monocytogenes* (22), *Histoplasma capsulatum* (9), and *T. cruzi* (41).

Our finding that virulent *F. tularensis* escapes the phagosome into the host cell cytoplasm has major implications for vaccine development. In the case of intracellular pathogens which reside exclusively within phagosomes in host cells, such as *Legionella pneumophila* and *M. tuberculosis* (15, 29), antigen presentation via major histocompatibility complex (MHC) class II molecules is favored and CD4 lymphocytes tend to play a dominant role in host defense. In the case of pathogens which exit the phagosome and reside freely in the host cell cytoplasm, such as *Listeria monocytogenes*, antigen presentation via MHC class I molecules is favored and CD8 lymphocytes tend to play a dominant role in host defense. We hypothesize that for vaccines against *F. tularensis* to be highly effective, they will need to be designed to allow the presentation of immunoprotective antigens via the MHC class I antigen presentation pathway.

ACKNOWLEDGMENTS

We thank Birgitta Sjostrand and Matthew Schibler for expert technical assistance.

This work was supported by grants AI053403 and HL077000 from the National Institutes of Health and grant DAMD17-03-1-0052 from the U.S. Army Medical Research and Materiel Command.

REFERENCES

1. **Anderson, R. G., J. R. Falck, J. L. Goldstein, and M. S. Brown.** 1984. Visualization of acidic organelles in intact cells by electron microscopy. Proc. Natl. Acad. Sci. USA **81:**4838–4842.
2. **Anthony, L., R. Burke, and F. Nano.** 1991. Growth of *Francisella* spp. in rodent macrophages. Infect. Immun. **59:**3291–3296.
3. **Antoine, J.-C., E. Prina, C. Jouanne, and P. Bongrand.** 1990. Parasitophorous vacuoles of *Leishmania amazonensis*-infected macrophages maintain an acidic pH. Infect. Immun. **58:**779–787.
4. **Armstrong, J. A., and P. D. Hart.** 1971. Response of cultured macrophages to *Mycobacterium tuberculosis* with observations on fusion of lysosomes with phagosomes. J. Exp. Med. **134:**713–740.
5. **Bell, J. F., C. R. Owen, and C. L. Larson.** 1955. Virulence of *Bacterium tularense.* I. A study of the virulence of *Bacterium tularense* in mice, guinea pigs, and rabbits. J. Infect. Dis. **97:**162–166.
6. **Bermudez, L. E., L. S. Young, and H. Enkel.** 1991. Interaction of *Mycobacterium avium* complex with human macrophages: roles of membrane receptors and serum proteins. Infect. Immun. **59:**1697–1702.
7. **Blackwell, J. M., R. A. B. Ezekowitz, M. B. Roberts, J. Y. Channon, R. B. Sim, and S. Gordon.** 1985. Macrophage complement and lectin-like receptors bind *Leishmania* in the absence of serum. J. Exp. Med. **162:**324–331.
8. **Buddingh, G. J., and F. C. Womack, Jr.** 1941. Observations on the infection of chick embryos with *Bacterium tularense*, *Brucella*, and *Pasteurella pestis*. J. Exp. Med. **74:**213–222.
9. **Bullock, W. E., and S. D. Wright.** 1987. Role of the adherence-promoting receptors CR3, LFA-1, and p150,95 in binding of *Histoplasma capsulatum* by human macrophages. J. Exp. Med. **165:**195–210.
10. **Burke, D. S.** 1977. Immunization against tularemia: analysis of the effectiveness of live *Francisella tularensis* vaccine in prevention of laboratory-acquired tularemia. J. Infect. Dis. **135:**55–60.
11. **Burton, P. R., N. Kordova, and D. Paretsky.** 1971. Electron microscopic studies of the rickettsia *Coxiella burnetii*: entry, lysosomal response, and fate of rickettsial DNA in L-cells. Can. J. Microbiol. **17:**143–150.
12. **Clemens, D. L., and M. A. Horwitz.** 1995. Characterization of the *M. tuberculosis* phagosome and evidence that phagosomal maturation is inhibited. J. Exp. Med. **181:**257–270.
13. **Clemens, D. L., B.-Y. Lee, and M. A. Horwitz.** 2000. Deviant expression of Rab5 on phagosomes containing the intracellular pathogens *Mycobacterium tuberculosis* and *Legionella pneumophila* is associated with altered phagosomal fate. Infect. Immun. **68:**2671–2684.
14. **Clemens, D. L., B.-Y. Lee, and M. A. Horwitz.** 2000. *Mycobacterium tuberculosis* and *Legionella pneumophila* phagosomes exhibit arrested maturation despite acquisition of Rab7. Infect. Immun. **68:**5154–5166.
15. **Clemens, D. L., B. Lee, and M. A. Horwitz.** 2002. The *Mycobacterium tuberculosis* phagosome in human macrophages is isolated from the host cell cytoplasm. Infect. Immun. **70:**5800–5807.
16. **Clerc, P. L., A. Ryter, J. Mounier, and P. J. Sansonetti.** 1987. Plasmid-mediated killing of eucaryotic cells by *Shigella flexneri* as studied by infection of J774 macrophages. Infect. Immun. **55:**521–527.

17. **Councilman, W. T., and R. P. Strong.** 1921. Plague-like infections in rodents. Trans. Assoc. Am. Phys. **36:**135–143.
18. **Crowle, A., R. Dahl, E. Ross, and M. May.** 1991. Evidence that vesicles containing living virulent *Mycobacterium tuberculosis* or *Mycobacterium avium* in cultured human macrophages are not acidic. Infect. Immun. **59:** 1823–1831.
19. **Dennis, D., T. Inglesby, D. Henderson, J. Bartlett, M. S. Ascher, E. Eitzen, A. Fine, A. Friedlander, J. Hauer, M. Layton, S. Lillibridge, J. McDade, M. Osterholm, T. O'Toole, G. Parker, T. M. Perl, P. K. Russel, and K. Tonat.** 2001. Tularemia as a biological weapon: medical and public health management. Working Group on Civilian Biodefense. JAMA **285:**2763–2773.
20. **Desjardins, M., J. E. Celis, G. van Meer, H. Dieplinger, A. Jahraus, G. Griffiths, and L. A. Huber.** 1994. Molecular characterization of phagosomes. J. Biol. Chem. **269:**32194–32200.
21. **Desjardins, M., L. A. Huber, R. G. Parton, and G. Griffiths.** 1994. Biogenesis of phagolysosomes proceeds through a sequential series of interactions with the endocytic apparatus. J. Cell Biol. **124:**677–688.
22. **Dreverts, D. A., and P. A. Campbell.** 1991. Roles of complement and complement receptor type 3 in phagocytosis of *Listeria monocytogenes* by inflammatory mouse peritoneal macrophages. Infect. Immun. **59:**2645–2652.
23. **Fortier, A., D. Leiby, R. Narayanan, E. Asafoadjel, R. Crawford, C. Nacy, and M. Meltzer.** 1995. Growth of *Francisella tularensis* LVS in macrophages: the acidic intracellular compartment provides essential iron required for growth. Infect. Immun. **63:**1478–1483.
24. **Gaillard, J.-L., P. Berche, J. Mounier, S. Richard, and P. Sansonetti.** 1987. In vitro model of penetration and intracellular growth of *Listeria monocytogenes* in the human enterocyte-like cell line Caco-2. Infect. Immun. **55:**2822–2829.
25. **Golovliov, I., V. Baranov, Z. Krocova, H. Kovarova, and A. Sjoestedt.** 2003. An attenuated strain of facultative intracellular bacterium *F. tularensis* can escape the phagosome of monocytic cells. Infect. Immun. **71:**5940–5950.
26. **Griffiths, G., A. McDowall, R. Back, and J. Dubochet.** 1984. On the preparation of cryosections for immunocytochemistry. J. Ultrastruct. Res. **89:**65–78.
27. **Heinzen, R., M. Scidmore, D. Rockey, and T. Hackstadt.** 1996. Differential interaction with endocytic and exocytic pathways distinguish parasitophorous vacuoles of *Coxiella burnetii* and *Chlamydia trachomatis*. Infect. Immun. **64:**769–809.
28. **Hirsch, J. G., and M. E. Fedorko.** 1968. Ultrastructure of human leucocytes after simultaneous fixation with glutaraldehyde and osmium tetroxide and "post-fixation" in uranyl acetate. J. Cell Biol. **38:**615.
29. **Horwitz, M. A.** 1983. Formation of a novel phagosome by the Legionnaires' disease bacterium (*Legionella pneumophila*) in human monocytes. J. Exp. Med. **158:**1319–1331.
30. **Horwitz, M. A.** 1988. Intracellular parasitism. Curr. Opin. Immunol. **1:**41–46.
31. **Horwitz, M. A., and F. R. Maxfield.** 1984. Legionella pneumophila inhibits acidification of its phagosome in human monocytes. J. Cell Biol. **99:**1936–1943.
32. **Ito, M., K. Nishiyama, S. Hyodo, S. Shigeta, and T. Ito.** 1985. Weight reduction of thymus and depletion of lymphocytes of T-dependent areas in peripheral lymphoid tissues of mice infected with *F. tularensis.* Infect. Immun. **49:**812–818.
33. **Lai, X., I. Golovliov, and A. Sjostedt.** 2001. *Francisella tularensis* induces cytopathogenicity and apoptosis in murine macrophages via a mechanism that requires intracellular bacterial multiplication. Infect. Immun. **69:**4961–4964.
34. **Lepperdinger, G., B. Strobl, and G. Kreil.** 1998. HYAL2, a human gene expressed in many cells, encodes a lysosomal hyaluronidase with a novel type of specificity. J. Biol. Chem. **273:**22466–22470.
35. **Long, G., J. Oprandy, R. Narayanan, A. Fortier, K. Porter, and C. Nacy.** 1993. Detection of *Francisella tularensis* in blood by polymerase chain reaction. J. Clin. Microbiol. **31:**730–734.
36. **Mosser, D. M., and P. J. Edelson.** 1985. The mouse macrophage receptor for C3bi (CR3) is a major mechanism in the phagocytosis of *Leishmania* promastigotes. J. Immunol. **135:**2785–2789.
37. **Noguiera, N., and Z. Cohn.** 1976. Trypansoma cruzi: mechanism of entry and intracellular fate in mammalian cells. J. Exp. Med. **143:**1402–1420.
38. **Orci, L., M. Ravazzola, M. Amherdt, O. Madsen, A. Perrelet, J. Vassali, and R. Anderson.** 1986. Conversion of proinsulin to insulin occurs coordinately with acidification of maturing secretory vesicles. J. Cell Biol. **103:**2273–2281.
39. **Patki, V., J. Virbasius, W. S. Lane, B.-H. Toh, H. S. Shpener, and S. Corvera.** 1997. Identification of an early endosomal protein regulated by phosphatidylinositol 3-kinase. Proc. Natl. Acad. Sci. USA **94:**7326–7330.
40. **Payne, N. R., and M. A. Horwitz.** 1987. Phagocytosis of *Legionella pneumophila* is mediated by human monocyte complement receptors. J. Exp. Med. **166:**1377–1389.
41. **Rimoldi, M. T., A. J. Tenner, D. A. Bobak, and K. A. Joiner.** 1989. Complement component C1q enhances invasion of human mononuclear phagocytes and fibroblasts by *Trypanosoma cruzi* trypomastigotes. J. Clin. Investig. **84:** 1982–1989.
42. **Sansonetti, P. J., A. Ryter, P. Clerc, A. T. Maurelli, and J. Mounier.** 1986. Multiplication of *Shigella flexneri* within HeLa cells: lysis of the phagocytic vacuole and plasmid mediated contact hemolysis. Infect. Immun. **51:**461–469.
43. **Schlesinger, L. S., and M. A. Horwitz.** 1991. Phagocytosis of *M. leprae* by human monocyte-derived macrophages is mediated by complement receptors CR1 (CD35), CR3 (CD11b/CD18), and CR4 (CD11c/CD18) and interferon gamma activation inhibits complement receptor function and phagocytosis of this bacterium. J. Immunol. **147:**1983–1994.
44. **Schlesinger, L. S., and M. A. Horwitz.** 1990. Phagocytosis of leprosy bacilli is mediated by complement receptors CR1 and CR3 on human monocytes and complement component C3 in serum. J. Clin. Investig. **85:**1304–1311.
45. **Schlesinger, L. S., C. G. Bellinger-Kawahara, N. R. Payne, and M. A. Horwitz.** 1990. Phagocytosis of *Mycobacterium tuberculosis* is mediated by human monocyte complement receptors and complement component C3. J. Immunol. **144:**2771–2780.
46. **Simonsen, A., R. Lippe, S. Christoforidis, J.-M. Gaullier, A. Brech, J. Callaghan, B.-H. Toh, C. Murphy, M. Zerial, and H. Stenmark.** 1998. EEA1 links phosphatidylinositol 3-kinase function to Rab5 regulation of endosome fusion. Nature **394:**494–498.
47. **Slot, J., H. Geuze, S. Gigengack, G. Lienhard, and D. E. James.** 1991. Immuno-localization of the insulin regulatable glucose transporter in brown adipose tissue of the rat. J. Cell Biol. **113:**123–135.
48. **Tanowitz, H., M. Wittner, Y. Kress, and B. Bloom.** 1975. Studies of in vitro infection by Trypanosoma cruzi. I. Ultrastructural studies on the invasion of macrophages and L-cells. Am. J. Trop. Med. Hyg. **24:**25–33.
49. **White, J. D., J. R. Rooney, P. A. Prickett, E. B. Derrenbacher, C. W. Beard, and W. R. Griffith.** 1964. Pathogenesis of experimental respiratory tularemia in monkeys. J. Infect. Dis. **114:**277–283.
50. **Winkler, H. H.** 1990. Rickettsia species (as organisms). Annu. Rev. Microbiol. **44:**131–153.
51. **Wubbolts, R., M. Fernandez-Borja, L. Oomen, D. Verwoerd, H. Janssen, J. Calafat, A. Tulp, S. Dusseljee, and J. Neefjes.** 1996. Direct vesicular transport of MHC class II molecules from lysosomal structures to the cell surface. J. Cell Biol. **135:**611–622.
52. **Wyrick, P. B., and E. A. Brownridge.** 1978. Growth of *Chlamydia psittaci* in macrophages. Infect. Immun. **19:**1054–1060.

Editor: D. L. Burns